RSC Advances

ROYAL SOCIETY OF CHEMISTRY

www.rsc.org/advances

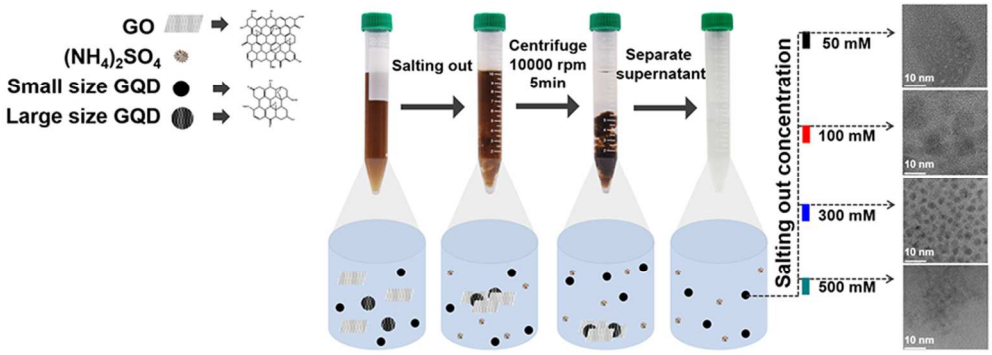

Schematic of graphene quantum dots salting-out procedure through ammonium sulfate
80x29mm (300 x 300 DPI)

RSC Advances

RSCPublishing

COMMUNICATION

Facile Method to Sort Graphene Quantum Dot by Size through Ammonium Sulfate Addition

Cite this: DOI: 10.1039/xoxxoooooox

Seongwoo Ryu,[a#] Kyueui Lee,[a#] Soon Hyung Hong[b,c] and Haeshin Lee[a,c*]

Received ooth January 2012,
Accepted ooth January 2012

DOI: 10.1039/xoxxoooooox

www.rsc.org/

We report a method to purify graphene quantum dots in its size simply by adding ammonium sulfate. The salt addition to a heterogeneous GQD suspension results in sorting GQD sub-populations with diameters of 2.7 ± 1.6, 5.1 ± 1.5, 13.3 ± 1.9, and 18.7 ± 4.4 nm, exhibiting different optical properties.

Since the discovery of graphene in 2004 [1, 2], it has received much attention due to its extraordinary mechanical, thermal, electrical [3-7] and bio-sensing abilities [8, 9]. Due to its metallic property, controlling the bandgap of graphene is a common research goal. It was theoretically predicted that a few nanometers of graphene, known as graphene quantum dots (GQDs), can exhibit bandgap properties similar to those of conventional semiconducting materials [10]. Afterward, GQDs were experimentally prepared, showing luminescence due to the presence of bandgaps [11-13]. The unique properties of GQD allow a variety of applications, including photovoltaic devices [14], organic light-emitting diodes [15], fuel cells [16] and biological imaging applications [17, 18].

Several methods have been reported to prepare GQDs. Nanolithography [19], hydro/solvothermal cutting [18, 20], electrochemical scissoring [14], chemical exfoliation [21], and the decomposition of fullerene [22] can all be used to produce GQDs. These methods can be divided into two categories. The first one includes methods that can prepare homogeneous GQDs in their dimension. However, they are not scalable. Nanolithography and the decomposition of fullerene are the methods belonging to this category. The second group includes methods that are scalable, but the dimensions of GQDs are heterogeneous. Hydro/solvothermal cutting, electrochemical scissoring and chemical exfoliation are examples of these methods. Comparing the scalability vs. the homogeneity of GQDs, scalability is the more important issue due to the aforementioned applications, but none of the previously developed methods can precisely control the dimensions of GQDs. The use of GQDs with a narrow distribution of their geometry can greatly improve the performance of GQD-containing devices. Most existing methods are able to produce GQDs with an average diameter of 4-6 nm. In addition, total synthesis of colloidally stable GQDs was reported [23]. The study used oxidative condensation reactions, but it requires repetition of synthesis and purification for multiple times to control the size of synthetic GQDs.

Preparation methods of homogeneous inorganic quantum dots in its dimension have been established [24]. Thus, development of an equivalent method for preparing GQDs with narrow size distribution is also important. Herein, we report a method that can prepare GQDs with narrow size distributions, and the distribution is controllable. We were able effectively to collect GQDs with average diameters of 2.7 ± 1.6, 5.1 ± 1.5, 13.3 ± 1.9, and 18.7 ± 4.4 nm (n = 60) for the first time without using a column. The ability to control the dimension of GQDs originates from the capability of a salt which can differentiate the solubility of individual GQDs. We used ammonium sulfate [$(NH_4)_2SO_4$] for GQD purification which is known as the most effective agent for protein salting-out according to Hofmeister series (Iyotropic series) [25].

[Anions] $SO_4^{2-} \approx F^- > HPO_4^{2-}$ > acetate > Cl^- > NO_3^- > Br^- > ClO_3^- > I^- > ClO_4^- > SCN^-

[Cations] $NH_4^+ > K^+ > Na^+ > Li^+ > Mg^{2+} > Ca^{2+}$ > guanidinium

The reason for choosing the salting-out method, which has been used by biologists for a long time [25], is molecular similarity between GQDs and a mixture of various proteins in some aspects. The first is the heterogeneity in size. CMG prepared by modified Hummer's method exhibits the heterogeneity in size, which corresponds to different molecular weight of each protein in the mixture. Furthermore, the molecular weight of GQD is similar compare to that of typical water-soluble small proteins. Considering the bond length of carbon [26], the estimated molecular weight of square-shaped, single-layered 10 nm GQD is approximately 30 kDa without considering the defect and functional groups of GQD. This value belongs to the molecular weight range (10 – 60 kDa) of a number of well-known water-soluble proteins such as lysozyme (~ 14 kDa),

green fluorescent proteins (~ 27 kDa), albumin (~ 66 kDa), etc. Also, a previous study reported that dialysis could be a method to separate GQDs [27], which has been widely used for protein purification, indicating that the dimension of GQDs is similar to water-soluble proteins. The second is the presence of charges on the edge of CMGs or on the surface of proteins. CMG oxidation results in the generation of 'hydrophilic' polar such as hydroxyl and carboxyl groups along its periphery, which is similar to the presence of polar amino acid residues such as glutamic acid and aspartic acid (i.e. R-COOH) as well as serine and threonine (R-OH). Furthermore, there are hydrophobic, carbon-rich amino acids for example, isoleucine, valine, phenylalanine, and tryptophane, which is similar to the presence of benzene and other carbon-rich regions in CMG. Recently, some studies demonstrated that the co-existence of hydrophilic and hydrophobic domains results in conformational changes of CMG similar to protein folding depending upon its salinity [28, 29]. In general, for the case of protein purification, large (i.e. high MW) and hydrophobic proteins are salted out first at a low concentration of $(NH_4)_2SO_4$, and then small (i.e. low MW) hydrophilic ones are precipitated out later at a high concentration. Similarly, we can expect that large, hydrophobic CMGs can be precipitated first followed by small, hydrophilic GQDs might be salted out at a later stage. Due to the predominant existence of hydrophilic groups at the edge of GQDs [30], the contribution from the hydrophilic edge might become dominant when the GQD size is reduced, resulting in an increase in the solubility of the GQDs.

We purified a colloidal GQD sub-population from a heterogeneous chemically modified graphene (CMG) suspension synthesized by a modified Hummer's method (first tube, Figure 1(a)). Figure 1(a) illustrates the role of ammonium sulfate. Its first role is the removal of large CMG flakes (> 50 nm) simply by the addition of a low concentration of ammonium sulfate (50 mM) (second tube). This concentration of ammonium sulfate effectively causes the immediate aggregation of large flakes of CMG, i.e., graphene oxides. The agglomerated CMGs can easily be removed by centrifugation (10,000 rpm for 5 min) (third tube). After this centrifugation, a suspension of very small yet heterogeneous GQDs was obtained (fourth tube). The second role of the ammonium sulfate is to sort the sizes of the GQDs by changing the final concentration. The detailed results are given in Figure 2. Briefly, we found that overall, the sizes of the GQDs decreased as the salt concentration was increased (TEM images, Figure1 (a)). Each sub-population was collected simply by adding different concentrations of ammonium sulfate. The unwanted, large GQDs were precipitated by the aforementioned 'salting-out' effect, which can be removed by centrifugation. Finally, the supernatant was dialyzed in water.

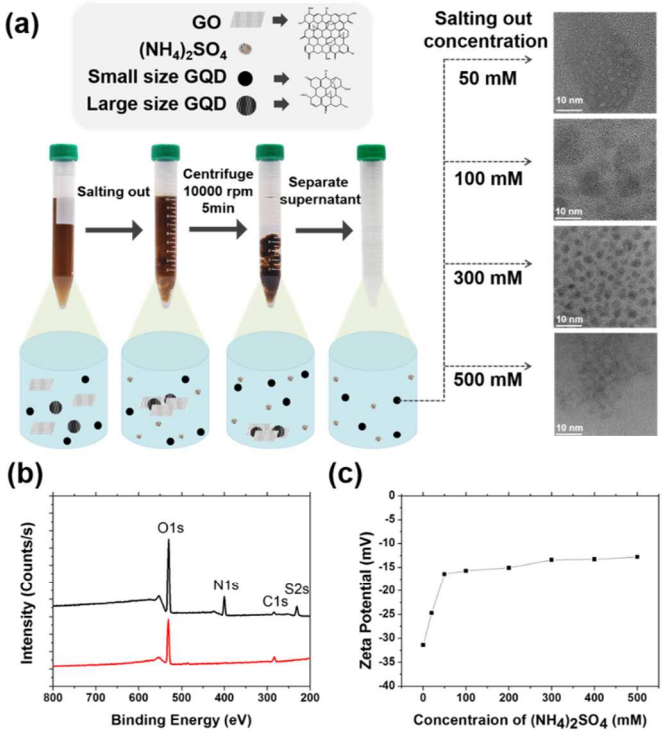

Figure 1. Schematic of the GQD salting-out procedure: (a) First, the CMG solution was prepared (first tube), after which the salt was added (second tube). Centrifugation was then conducted (third tube), after which the supernatant solution was obtained (fourth tube). As the salt concentration increases, smaller GQDs are purified from the supernatant. (b) XPS spectra of GQDs before (black) and after dialysis (red) to remove the added salt. After removing the salt, N1s and S2s peaks from the salt were not observed. (c) Zeta potential of GQDs as a function of the salt concentration. The zeta potential value was increased to -16.4mV (up to 50 mM), after which it did not change throughout the entire salting-out scale.

To examine the ammonium sulfate contamination, we utilized X-ray photoelectron spectroscopy (XPS). Figure 1(b) shows the GQD flakes before and after dialysis to discern the presence of ammonium sulfate. Before dialysis, the nitrogen 1s photoelectron (N1s) peak appeared around 400.0 eV and the sulfur 2p (S2p) peak appeared at 231.5 eV from the salt, $(NH_4)_2SO_4$ (black). However, the characteristic salt peaks completely disappeared after dialysis (red). This result indicates that the purified GQDs do not contain residual salt ions, which can act as a contaminant. The minor degree of interaction between the GQDs and the salt as demonstrated by the XPS results was further demonstrated by the zeta potential (Figure 1(c)). Each purified GQD sample (GQD50, GQD100, GQD300, and GQD500) showed a similar level of negative charge, ~15 mV, with a slight tendency of an increase in the zeta potential from -16.4 mV (GQD50) to - 12.8 mV (GQD500). Throughout this study, GQD100 represents the GQDs purified by adding 100 mM of ammonium sulfate. Likewise, the GQDs purified with 500 mM of ammonium sulfate are referred to as GQD500.

The purified GQD sub-populations exhibited differences in their chemical compositions, in other words, in their functional groups (Figure S1). The high-resolution C1s spectra showed differences in the carbon chemistries between the GQD50 and GQD100 samples. The major C-C photoelectron peak which appeared at 284.5 eV was more significant in GQD100 (second, red) than that in GQD50 (first, black). The increased C-C photoelectron peak was unchanged for the

GQDs purified with higher concentrations of ammonium sulfate (blue for GQD300 and green for GQD500). In general, large GO or GQD (> 20 nm) show higher oxidative levels than nano-sized GQDs smaller than 4 nm. In particular, the oxidation of GQDs primarily appears at the edge with functional carboxyl or hydroxyl groups (Figure S1). The reason for the edge distribution of the functional groups may be the preferential chemical cleavage toward an on-plane oxygen-containing functional group, such as an epoxide or a carbonyl group [20, 31]. After the cleavage, oxygen-containing functional group, such as hydroxyl and carbonyl groups are located alongside at the edge of GQDs. Therefore, the charges in GQDs are found mainly along the periphery (Figure S2(a)). Also, as the internal core region of GQDs is relatively hydrophobic, the overall charge density increases when the size of GQDs gets smaller (Figure S2(b)).

Raman spectroscopy was also used to characterize the vibrational modes of the GQDs (Figure S3). The Raman spectrum of the GQDs after salting-out exhibited the D-band at 1354 cm^{-1} and the broad G-band at 1594 cm^{-1}. I_D/I_G values were gradually increased from 0.75 for GQD50, 0.78 for GQD100, 0.80 for GQD300, and 0.84 for GQD500. Considering the fact that GQDs were generated by preferential chemical cleavage along the defected, oxygenated areas, the edge GQDs is rich in oxygen-containing moieties, but the inside core is rich in graphitic carbon. Thus, when the size is decreased, I_G value is expected to decrease due to the increase in the edge perimeter length to core ratio. XRD experiments were also performed, but no significant differences were observed.

The TEM analysis demonstrated that the simple addition of the salt allowed the sorting out of the size of GQDs. Figure 2 shows TEM images of GQDs purified in the presence of $(NH_4)_2SO_4$ (50, 100, 300, and 500 mM); the corresponding size distributions are shown in the histograms. Representative TEM images for the sample purified in the presence of 50 mM of $(NH_4)_2SO_4$ (Figures 2(a) and (b)) exhibit mostly large, chemically modified graphene (CMG) and GQDs between 10 – 20 nm in size with a population distribution of approximately 70%, with the remaining 30% larger than 20 nm (18.7 nm on average with standard deviation (SD) of 4.4 nm, n = 60). As the salt concentration increases, homogeneous, small GQDs were obtained (Figures 2(c) – (h)). For GQD100, the sizes of GQDs were 13.3 nm on average with SD of 1.9 nm (n = 60) (Figure 2(c) and (d)), while for GQD300, the average size was 5.1 nm with SD of 1.5 nm (n = 60) (e and f). Finally, for GQD500, the average size was 2.7 nm with SD of 1.6 nm (n = 60) (g and h). Atomic force microscopy (AFM) height profiles confirmed the thicknesses of the purified GQDs (Figure S4). Previously, GQDs with a large diameter (> 22 nm) showed multiple layers (more than five layers) to some degree [27]. However, multi-layer GQDs were not observed here. It has been reported that the height of single-layer graphene can vary from 0.3 to 1.6 nm according to AFM measurements [1, 32, 33]. According to the AFM height profiles in this study, most of the GQD particles purified by 500 and 300mM of $(NH_4)_2SO_4$ showed AFM height profiles of approximately 0.8 nm, indicating one layer of graphene (Figures S4(a)-(d)). Note that the lateral sizes of the purified GQDs were similar between the samples. In general, the tip geometry causes the inaccuracy in lateral size determination particularly for the small nanoparticles. The relatively large GQD samples of GQD50 and GQD100 showed one to two layers of graphene (Figures S4(e)-(h)). The difference in the number of graphene layers can be another advantage of the salting-out method over existing methods currently used to prepare GQDs. Figure 2(i) shows comparative histogram histograms of the size distributions of GQDs after the proposed salting-out method (bottom) and after chemical exfoliation (purple) [21, 34], electrochemical scissoring (blue) [14, 35], solvothermal cutting (green) [18, 36], and hydrothermal cutting (red) [20, 37]. In general, most GQD synthesizing methods show either wide-ranging heterogeneous distributions (e.g., hydrothermal cutting) or narrow-range yet uncontrollable size distributions. In detail, the hydrothermal cutting method led to GQDs of 1 to 16 nm in size, while the other methods showed size distributions of less than 10 nm. Importantly, the salting-out method was able to control the size of the GQDs depending on the salt concentration.

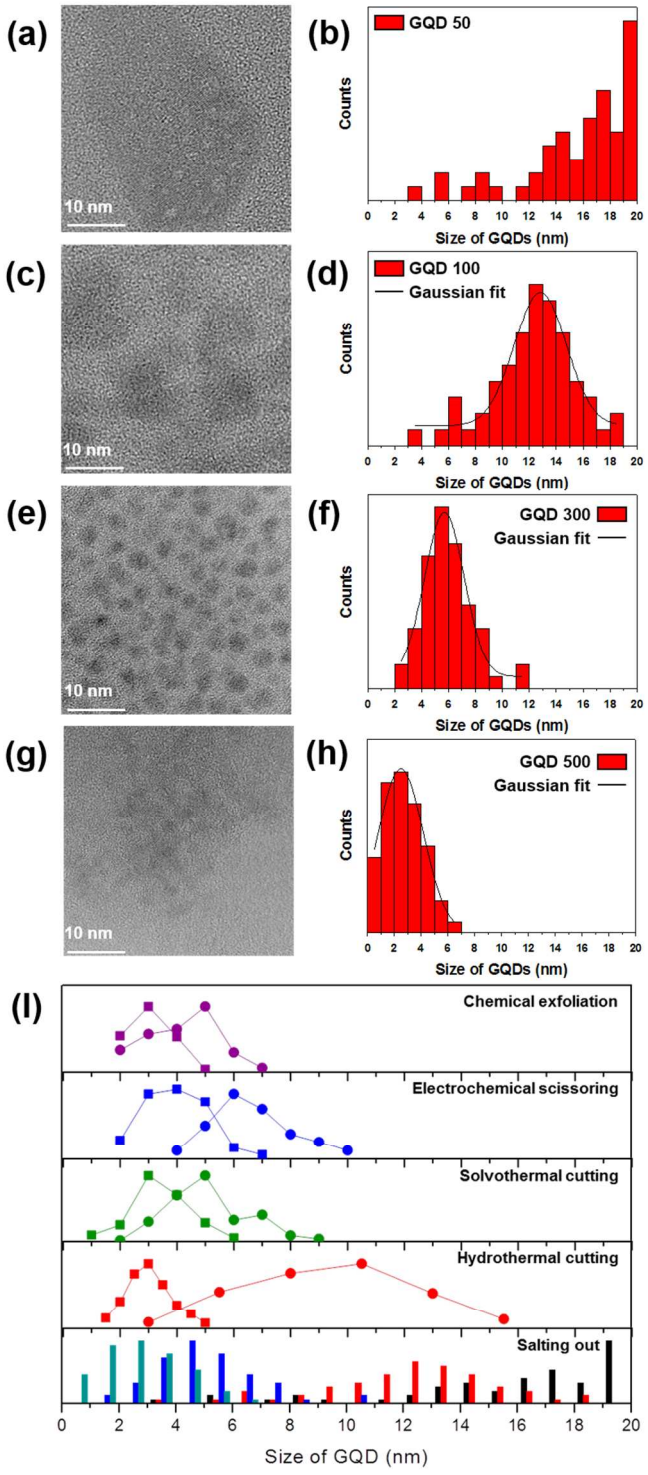

Figure 2. Size distribution of the purified GQDs: (a). A typical TEM image of GQD50 and its corresponding size distribution (b). (c) A TEM image of GQD100 and its corresponding size distribution (d). (e) A TEM image of GQD300 and its corresponding distribution (f). (g) A TEM image of GQD500 and its corresponding size distribution (h). (n = 60) (i) Overall histograms of samples purified by the salting-out process: GQD50 (black), GQD100 (red), GQD300 (blue), GQD500 (green) and comparisons with various GQD synthesizing methods.

The high-resolution TEM (HRTEM) results showed that the edge structures of the purified GQD have both zigzag (red lines in Figure 3(b) and (c)) and armchair (blue lines in Figure 3(b) and (c)) configurations. Each edge structure is determined by the bandgap energy and thus defines the optical properties. In general, the bandgap energy rapidly decays to zero eV for the zigzag edge, and it slowly approaches zero eV for the armchair edge [38]. As the purified GQDs have both types of edge structures, the optical properties can predominantly be determined by their individual sizes. Due to the quantum confinement effect [12, 39], the energy bandgap of GQDs is approximately related to the inverse proportion of their sizes. Previously, the largest bandgap value of approximately 3 eV was achieved by reducing the size of the GQDs [20, 38]. Figure 3(d) shows the UV-Vis spectrophotometry absorption results of the GQDs. The salting-out GQDs exhibited wide n-π* transition ranges from 290 nm to 332 nm, which corresponds to 3.85 eV (332 nm) and 4.27 (290 nm).

Salts other than $(NH_4)_2SO_4$ that are chosen from Hofmeister's series resulted in salting-out phenomenon, but the degree of salting-out is not as effective as $(NH_4)_2SO_4$. Experiments using salts such as ammonium acetate (NH_4OAc), ammonium chloride (NH_4Cl), and ammonium nitrate (NH_4NO_3) demonstrated that $(NH_4)_2SO_4$ showed the best efficiency in salting-out ($(NH_4)_2SO_4$ > NH_4OAc > NH_4Cl), which agreed with the Hofmeister's series (Figure S5(a)). A similar result was obtained for using a series of sodium salts: sodium sulphate (Na_2SO_4), sodium phosphate ($NaHPO_4$), sodium acetate (NaOAc), sodium chloride (NaCl), sodium nitrate ($NaNO_3$), and sodium iodate (NaI). The concentration of all used salts were fixed to 50 mM. As expected, a fraction of hydrophobic CMGs in the heterogeneous mixture began to be salted out even utilizing the sodium-containing salts. However, the efficiency of salting-out decreased compared to that of ammonium sulphate: $(NH_4)_2SO_4$ > Na_2SO_4 > $NaHPO_4$ > NaOAc > NaCl > $NaNO_3$ > NaI (Figure S5(b)). This result showed that any salt in Hofmeister's series generally exhibited dehydration from macromolecular solutes resulting in salting-out. Characterization of physicochemical properties of each precipitant and supernatant from each salt can be a topic for further study.

As the sizes of GQDs were reduced (i.e., purified under a high salt condition), the absorption peak was blue-shifted, showing a large amount of bandgap energy [39-41]. This also resulted in large differences in the photoluminescence (PL) emissions (Figures 3(e) and (f)). The purified GQDs exhibited emissions of 596 nm for GQD50, 515 nm for GQD100, 486 nm for GQD300, and 477 nm for GQD500 when the samples were placed under a 312 nm UV lamp. We also found absorption at 402 nm and 436 nm for the GQD100, 300, and 500 samples, which can be interpreted as the PL from the remaining oxidative functional groups and the mixed edge structures considering previous theoretical calculations [12, 39].

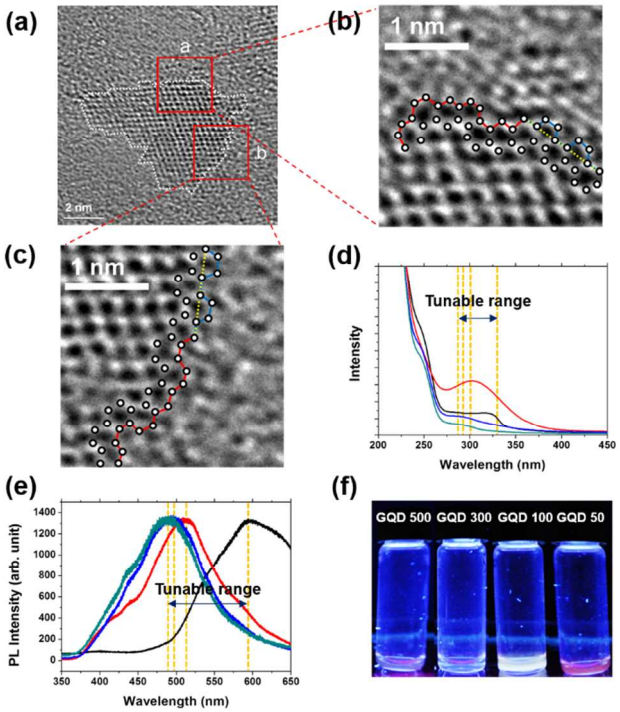

Figure 3. (a) TEM images of purified GQDs and magnified images to examine the edge structures. (b) Location 'a' and (c) location 'b'. (b and c) The red lines indicate the zigzag edges of the GQDs, and the blue lines show the armchair edges of the GQDs. (d) UV-Vis absorption results (Abs) of the GQD50 (black), GQD100 (red), GQD300 (blue), and GQD500 (green) supernatants from CMG suspensions and (e) their PL spectra (E_{ex} = 325 nm). (f) GQD suspension placed on a 312 nm UV lamp: from the left GQD500, GQD300, GQD100 and GQD50

Conclusions

We demonstrated for the first time that a simple addition of ammonium sulfate can be a scalable means of purifying GQDs with diameters from 2.7 to 18.7 nm. This method does not require any type of column for purification. Depending on the salt concentration, the sizes of the GQDs can be controlled with a narrow distribution, exhibiting bandgaps ranging from 3.85 eV to 4.27 eV with spectral emissions ranging from 402 nm 596 nm. The scalable purification method using the salting-out process introduced here will play an important role in providing high-quality GQDs for various applications related to GQDs.

Acknowledgements

The authors acknowledge the financial support from National Research Foundation of South Korea: Mid-career scientist grant (2014002855). This work is also supported in part from Center for Nature-inspired Technology (CNiT) in KAIST Institute for NanoCentury (KINC) and World Premier Materials from the Ministry of Industry, Trade, and Natural Resources. S. Ryu and K. Lee equally contributed to this work (#).

Notes and references

[a]Department of Chemistry, [b]Department of Materials Science and Engineering, Korea Advanced Institute of Science and Technology (KAIST), 291 University Rd. Daejeon 305-701, Republic of Korea [c]Center for Nature-inspired Technology (CNiT) in KAIST Institute for NanoCentury, Korea Advanced

Institute of Science and Technology (KAIST), 291 University Rd. Daejeon 305-701, Republic of Korea
Electronic Supplementary Information (ESI) available: [details of any supplementary information available should be included here]. See DOI: 10.1039/c000000x/

1 K. S. Novoselov, A. K. Geim, S. V. Morozov, D. Jiang, Y. Zhang, S. V. Dubonos, I. V. Grigorieva and A. A. Firsov, *Science*, 2004, **306**, 666.
2 A. K. Geim and K. S. Novoselov, *Nat. Mater.*, 2007, **6**, 183.
3 C. G. Lee, X. D. Wei, J. W. Kysar and J. Hone, *Science*, 2008, **321**, 385.
4 A. A. Balandin, S. Ghosh, W. Bao, I. Calizo, D. Teweldebrhan, F. Miao and C. N. Lau, *Nano Lett.*, 2008, **8**, 902.
5 A. H. Castro Neto, F. Guinea, N. M. R. Peres, K. S. Novoselov and A. K. Geim, *Rev. Mod. Phys.,* 2009, **81**, 109.
6 S. Stankovich, D. A. Dikin, R. D. Piner, K. A. Kohlhaas, A. Kleinhammes, Y. Jia, Y. Wu, S. T. Nguyen and R. S. Ruo□, *Carbon*, 2007, **45**, 1558.
7 T. Schwamb, B. R. Burg, N. C. Schirmer and D. Poulikakos, *Nanotechnology*, 2009, **20**, 405704.
8 S. Alwarappan, A. Erdem, C. Liu and C.-Z. Li, *J. Phys. Chem. C*, 2009, **113**, 8853.
9 S. Alwarappan, C. Liu, A. Kumar and C.-Z. Li, *J. Phys. Chem. C*, 2010, **114**, 12920.
10 P. G. Silvestrov and K. B. Efetov, *Phys. Rev. Lett.*, 2007, **98**, 016802.
11 C. Ö. Girit, J. C. Meyer, R. Erni, M. D. Rossell, C. Kisielowski, L. Yang, C.-H. Park, M. F. Crommie, M. L. Cohen, S. G. Louie and A. Zettl, *Science*, 2009, **323**, 1705.
12 K. A. Ritter and J. W. Lyding, *Nat. Mater.*, 2009, **8**, 235.
13 J. Shen, Y. Zhu, X. Yang and C. Li, *Chem. Commun.*, 2012, **48**, 3686.
14 Y. Li, Y. Hu, Y. Zhao, G. Shi, L. Deng, Y. Hou and L. Qu, *Adv. Mater.*, 2011, **23**, 776.
15 L. Tang, R. Ji, X. Cao, J. Lin, H. Jiang, X. Li, K. S. Teng, C. M. Luk, S. Zeng, J. Hao and S. P. Lau, *ACS Nano*, 2012, **6**, 5102.
16 Y. Li, Y. Zhao, H. Cheng, Y. Hu, G. Shi, L. Dai and L. Qu, *J. Am. Chem. Soc.*, 2012, **134**, 18932.
17 X. Sun, Z. Liu, K. Welsher, J. T. Robinson, A. Goodwin, S. Zaric and H. Dai, *Nano Res.*, 2008, **1**, 20312.
18 S. J. Zhu, J. H. Zhang, C. Y. Qian, S. J. Tang, Y. F. Li, W. J. Yuan, B. Li, L. Tian, F. Liu, R. Hu, H. N. Gao, H. T. Wei, H. Zhang, H. C. Sun and B. Yang, *Chem. Commun.*, 2011, **47**, 6858.
19 L. A. Ponomarenko, F. Schedin, M. I. Katsnelson, R. Yang, E. W. Hill, K. S. Novoselov and A. K. Geim, *Science*, 2008, **320**, 356.
20 D. Pan, J. Zhang, Z. Li and M. Wu, *Adv. Mater.*, 2010, **22**, 734.
21 J. Peng, W. Gao, B. K. Gupta, Z. Liu, R. Romero-Aburto, L. H. Ge, L. Song, L. B. Alemany, X. B. Zhan, G. H. Gao, S. A. Vithayathil, B. A. Kaipparettu, A. A. Marti, T. Hayashi, J.-J. Zhu and P. M. Ajayan, *Nano Lett.*, 2012, **12**, 844.
22 J. Lu, P. S. E. Yeo, C. K. Gan, P. Wu and K. P. Loh, *Nat. Nanotechnol.*, 2011, **6**, 247.
23 X. Yan, X. Cui and L. Li, *J. Am. Chem. Soc.*, 2010, **132**, 5944.
24 B. O. Dabbousi, J. Rodriguez-Viejo, F. V. Mikulec, J. R. Heine, H. Mattoussi, R. Ober, K. F. Jensen and M. G. Bawendi, *J. Phys. Chem. B*, 1997, **101**, 9463.
25 P. K. Grover and R. L. Ryall, *Chem. Rev.*, 2005, **105**, 1.
26 D. R. Lide, *Tetrahedron*, 1962, **17**, 125.
27 S. Kim, S. W. Hwang, M.-K. Kim, D. Y. Shin, D. H. Shin, C. O. Kim, S. B. Yang, J. H. Park, E. Hwang, S.-H. Choi, G. Ko, S. Sim, C. Sone, H. J. Choi, S. Bae and B. H. Hong, *ACS Nano*, 2012, **6**, 8203.
28 R. L. D. Whitby, A. Korobeinyk, V. M. Gun'ko, R. Busquets, A. B. Cundy, K. László, J. Skubiszewska-Zieba, R. Leboda, E. Tombacz, I. Y. Toth, K. Kovacs and S. V. Mikhalovsky, *Chem. Commun.*, 2011, **47**, 9645.
29 R. L. D. Whitby, V. M. Gun'ko, A. Korobeinyk, R. Busquets, A. B. Cundy, K. Laszlo, J. Skubiszewska-Zieba, R. Leboda, E. Tombacz, I. Y. Toth, K. Kovacs and S. V. Mikhalovsky, *ACS Nano*, 2012, **6**, 3967.
30 Y. Q. Dong, J. W. Shao, C. Q. Chen, H. Li, R. X. Wang, Y. W. Chi, X. M. Lin and G. N. Chen, *Carbon*, 2012, **50**, 4738.
31 J.-L. Li, K. N. Kudin, M. J. McAllister, R. K. Prud'homme, I. A. Aksay and R. Car, *Phys. Rev. Lett.*, 2006, **96**, 176101.
32 A. Gupta, G. Chen, P. Joshi, S. Tadigadapa and P. C. Eklund, *Nano Lett.*, 2006, **6**, 2667.
33 C. Casiraghi, A. Hartschuh, E. Lidorikis, H. Qian, H. Harutyunyan, T. Gokus, K. S. Novoselov and A. C. Ferrari, *Nano Lett.*, 2007, **7**, 2711.
34 L.-L. Li, J. Ji, R. Fei, C.-Z. Wang, Q. Lu, J.-R. Zhang, L.-P. Jiang and J.-J. Zhu, *Adv. Funct. Mater.*, 2012, **22**, 2971.
35 M. Zhang, L. L. Bai, W. H. Shang, W. J. Xie, H. Ma, Y. Y. Fu, D. C. Fang, H. Sun, L. Z. Fan, M. Han, C. M. Liu and S. H. Yang, *J. Mater. Chem.*, 2012, **22**, 7461.
36 S. J. Zhu, J. H. Zhang, X. Liu, B. Li, X. F. Wang, S. J. Tang, Q. N. Meng, Y. F. Li, C. Shi, R. Hu and B. Yang, *RSC Adv.*, 2012, **2**, 2717.
37 D. Y. Pan, L. Guo, J. C. Zhang, C. Xi, Q. Xue, H. Huang, J. H. Li, Z. W. Zhang, W. J. Yu, Z. W. Chen, Z. Li and M. H. Wu, *J. Mater. Chem.*, 2012, **22**, 3314.
38 A. D. Güçlü, P. Potasz, P. Hawrylak, *Phys. Rev. B*, 2010, 82, 155445.
39 Z. Z. Zhang and K. Chang, *Phys. Rev. B: Condens. Matter Mater. Phys.*, 2008, **77**, 235411.
40 H. T. Li, X. D. He, Z. H. Kang, H. Huang, Y. Liu, J. L. Liu, S. Y. Lian, C. H. A. Tsang, X. B. Yang and S. T. Lee, *Angew. Chem., Int. Ed.*, 2010, **49**, 4430.
41 R. Q. Zhang, E. Bertran and S.-T. Lee, *Diamond Relat. Mater.*, 1998, **7**, 1663.